LANGMUIR

pubsiacs.org/Langmuir Article

Molecular Dynamics and Surface Interactions of Nickelocene Adsorbed on Silica: A Paramagnetic Solid-State NMR Study

Jordon W. Benzie, Gabrielle E. Harmon-Welch, John C. Hoefler, Vladimir I. Bakhmutov,* and Janet Blümel*



Cite This: Langmuir 2022, 38, 7422-7432



ACCESS I

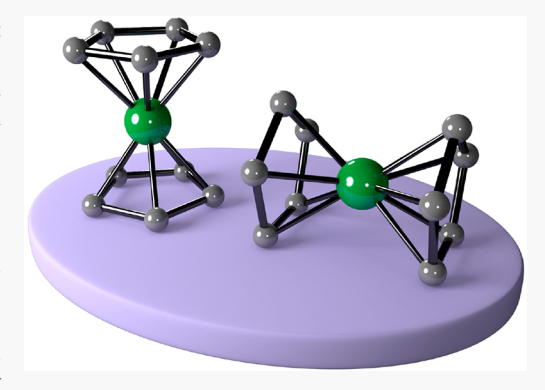
Metrics & More

Article Recommendations



Supporting Information

ABSTRACT: When grinding nickelocene with silica in the absence of a solvent at room temperature, it adsorbs on the surface within the pores. This has also been demonstrated visually by adsorbing green nickelocene in the pores of a large colorless silica gel specimen. While this dry adsorption and translational mobility of nickelocene within the pores is proven visually, the site-to-site mobility of the nickelocene molecules and their orientation toward the surface are not yet understood. In this contribution, mesoporous silica is used as the support material for a systematic solid-state NMR study of these issues. Paramagnetic ¹H VT solid-state NMR and T₁ relaxation times have been powerful tools for studying the dynamics of nickelocene on the silica surface. Herewith, the mobility of the surface-adsorbed nickelocene molecules in the pores could be quantified on the molecular scale. According to the obtained data, the nickelocene molecules move like a liquid on the surface. Isotropically



moving molecules exchange places rapidly with surface-attached molecular states of nickelocene in a sample with submonolayer surface coverage. This finding is corroborated by a macroscopic visualization experiment. The states of the surface-attached horizontally oriented nickelocene molecules that are prevalent at temperatures below 200 K have been quantified. The temperature dependencies of the rate k in coordinates of $\ln(k)$ versus 1/T and $\ln(k/T)$ versus 1/T form ideal straight lines that allow the determination of the kinetic parameters $E_{\rm act} = 5.5$ kcal/mol, $A = 1.1 \times 10^{10}$, $\Delta H^{\ddagger} = 5.0$ kcal/mol, and $\Delta S^{\ddagger} = -15$ eu. Investigating a sample with equal amounts of nickelocene and ferrocene in a submonolayer amount of 80% overall surface coverage shows that the different metallocenes mix on the molecular level on the silica surface.

INTRODUCTION

Understanding the adsorption of small molecules on surfaces is equally important for large processes in industry and experiments in academia that involve the separation sciences and catalysis. However, solid-state NMR spectroscopic 1-3 adsorption studies involving solid supports have focused mainly on liquids such as water, alcohols, and benzene.⁴ NMR spectroscopic analyses of surface-adsorbed solids are rare. 5-7 For example, complexes with aromatic ligands have been adsorbed on silica⁸ and studied by ¹³C solid-state NMR.

Recently, our group described that crystalline solids like phosphine oxides⁵⁻⁷ can be adsorbed on diverse surfaces by manual grinding of the adsorbate and support material with a mortar and pestle. Subsequently, the adsorbed species have been investigated by solid-state NMR, and their modes of mobility on the surfaces have been quantified. When phosphine oxides are adsorbed on silica surfaces,⁹ the oxygen of the P=O group hydrogen-bonds with silanol groups. 10 Molecular adducts of P=O groups with silanols, 10 hydrogen peroxide, 11-13 and di(hydroperoxy)alkanes 12-16 have all been identified by single-crystal X-ray diffraction, and the presence of hydrogen bonds has been proven.

Solid-state NMR spectroscopy¹⁻³ is the most powerful method to investigate species bound to amorphous support materials, for example, immobilized catalysts on support surfaces.3 In this context, the most important anisotropic interactions in solids are the chemical shift anisotropy (CSA) and dipolar interactions. 1,2 The CSA correlates with the electronic asymmetry around a nucleus. Spherically symmetric species like phosphonium salts have a small ³¹P CSA, ¹⁷ while the signals of polycrystalline phosphine oxides show a large CSA. 5-7 The latter manifests in solid-state NMR spectra as rotational sidebands in addition to the isotropic line in MAS (magic angle spinning) spectra. Anisotropic dipolar interactions typically lead to a broadening of the solid-state NMR signals. In solution all anisotropic interactions are averaged out, and the narrow isotropic lines are obtained. Importantly, when

Received: February 6, 2022 May 20, 2022 Revised: Published: June 8, 2022





the mobility of a molecule is limited and only partial averaging out of anisotropic interactions occurs, the residual CSA and dipolar interactions can be exploited for studying dynamic effects. For example, one can gain insight into the mobility modes of a surface-adsorbed molecule, as described for nickelocene in the Results and Discussion section.

We communicated previously that metallocenes of the type Cp_2M (Cp = cyclopentadienyl, C_5H_5) self-adsorb on silica surfaces by mixing the dry components manually. ^{18–23} It has been shown with ferrocene that several modes of mobility exist. Translational movement in the pores could be visualized by bringing a large silica specimen in contact with a single crystal of ferrocene. ²¹ Spiraling movement on the surface within the pores leads to a reorientation of the ferrocene molecules with respect to the external magnetic field. ¹⁹ This movement substantially reduces the anisotropic interactions in the solid-state NMR spectra. For example, the CSA and even the large quadrupolar interactions are averaged out due to the mobility when measuring ²H NMR of adsorbed deuterated ferrocene. ²¹ At elevated temperatures, a temporary detachment from the surface also has to be considered.

In contrast to the above-mentioned adsorbed phosphine oxides, hydrogen bonding can be excluded for the interactions of the metallocenes with silica. They have to be van der Waals interactions, but the orientation of nickelocene in particular, standing upright or lying on its side at low temperature, with the Cp-Ni-Cp axis perpendicular or parallel to the surface, respectively, remains to be determined. Furthermore, it is still unclear whether other modes of mobility, such as tumbling or detachment from the surface, are present besides the obvious translational mode.

Under an inert atmosphere ferrocene does not undergo chemical reactions even with supports such as silica. 19,21-23 In contrast, the important polymerization catalysts of the type Cp₂MCl₂ react readily via the chloride ligands when they are supported on silica²⁴ or incorporated into polymers²⁵ or sol–gel-type materials.²⁶ But even in the absence of chloride ligands, some of the Cp2M metallocenes react quickly with oxide surfaces after the adsorption step. On a silica or alumina surface, chromocene forms the important heterogeneous Union Carbide catalyst that is used industrially for olefin polymerization under mild conditions in the absence of a cocatalyst.^{27,28} Despite the importance of this catalyst, its structure remains largely unknown. The commonly accepted partial structure of the catalytically active surface species consists of a CpCr(III) moiety that must be bound to a surface siloxide anion, as determined by solid-state NMR¹⁸ and XPS and IR studies.²⁷

For our group, the most important incentive to study the interactions of Cp_2M -type metallocenes adsorbed in monolayers with support surfaces is related to the potential creation of single atom catalysts (SACs) by reducing the metal center. Preliminary results for nickelocene (Cp_2Ni , (C_5H_5) $_2Ni$, 1), adsorbed in a monolayer on silica, showed that it can be reduced by hydrogen to form a SAC that, in contrast to 1, catalyzes the cyclotrimerization of phenylacetylene. Importantly with respect to later applications as SACs, when the adsorption of 1 is undertaken in the absence of a solvent, a well-defined monolayer is formed. No stacking of metallocenes in multiple layers on the surface occurs on any support. In case an excess of metallocene is offered, it remains in its polycrystalline form and does not adsorb. 19-23

Besides the application aspect, phenomenologically and for understanding the reactivity, the orientation of the nickelocene molecules with respect to the surface, whether their Cp–Ni–Cp axis is oriented perpendicular or parallel to the surface, is of interest. Polycrystalline nickelocene is reasonably stable at ambient temperature under an inert atmosphere and allows its characterization with paramagnetic NMR spectroscopy. $^{18,19,29-34}$ The same applies to 1 adsorbed on silica. 21

In this contribution, we apply variable-temperature 1 H solid-state NMR and T_1 relaxation time measurements to investigate the behavior of 1 on the surface in the pores of silica on the molecular scale. Both paramagnetic 1 H MAS and 1 H wide-line NMR spectroscopy will be employed at different temperatures. 1 H solid-state NMR spectroscopy without sample rotation has, for example, been successfully used recently to investigate the distribution of moisture in polymers. 35,36 The new insights gained on the different states of mobility of nickelocene on a silica surface should have major implications for single atom catalysis, as well-defined adsorption is the first step in generating these atom-economic and active heterogeneous catalysts. 37

■ RESULTS AND DISCUSSION

The most closely related diamagnetic analogue of nickelocene $(Cp_2Ni, 1)$ is ferrocene $(Cp_2Fe, 2)$. Recently, while working in the field of solid-state NMR studies of molecular dynamics on the surfaces of porous materials, we have found liquidlike behavior of ferrocene on a silica surface at moderate temperatures.²³ In the context of these studies, the mobility of nickelocene on the same silica surface is of great interest. Furthermore, in our quest to generate a nickel single atom catalyst from surface-adsorbed nickelocene, 21 a deeper knowledge about the interactions with the surface is essential. Most importantly, preliminary results regarding the dry adsorption of nickelocene on a silica surface²¹ have to be corroborated, and the behavior and orientation of the individual molecules on the surface have to be elucidated. More specifically, for the subsequent reduction of the nickelocene molecules with hydrogen it is important to know whether they stand "upright" on their Cp rings as pedestals or lie on the surface "sideways" like the axle and wheels of a car (graphical abstract).

According to preliminary data communicated earlier, ²¹ and judging from its ¹H NMR spectrum, compound 1 behaves similarly to ferrocene after adsorption on silica in a submonolayer. As compared to polycrystalline 1, the ¹H NMR signal of surface-adsorbed nickelocene displays a diminished chemical shift anisotropy (CSA). ²¹ However, the deeper reasons for this behavior and the solid-state characteristics of 1 have not been investigated yet.

In this study we apply both variable temperature (VT) ¹H wide-line and MAS NMR to characterize neat polycrystalline nickelocene (1). All samples have been prepared by dry adsorption ^{19–23} of 1 on a silica surface. The adsorption of 1 is fast and complete within a few minutes when silica and nickelocene are mixed or gently grinded together with a mortar and pestle. No physical reaction takes place, and the adsorbed nickelocene can be washed off completely with THF (Figure S1). When bringing a large silica specimen into contact with polycrystalline nickelocene, it takes a few hours to obtain maximal saturation with a monolayer of 1.

When polycrystalline nickelocene is placed on top of silica powder and left undisturbed, the adsorption progresses within days (Figure 1). In this case, either the nickelocene could

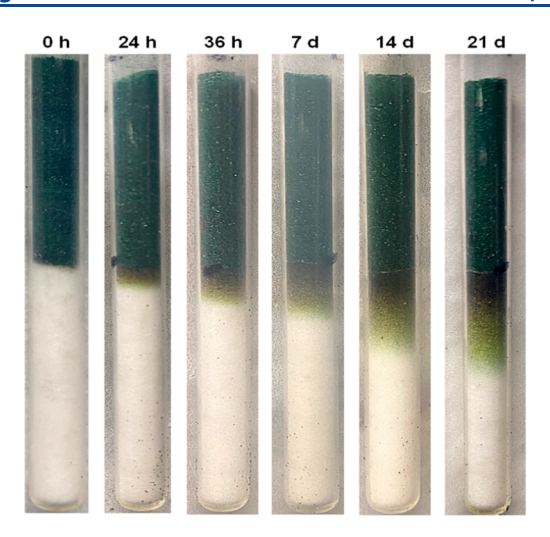


Figure 1. Polycrystalline nickelocene (1) migrates into silica during the indicated times when it is placed on top of it.

slowly transition from one silica particle to the next via contact points or it could migrate through the gas phase because 1 is fairly volatile. The latter assumption is corroborated by the following experiment. When polycrystalline nickelocene is placed into a vial that opens in the direction of a large silica gel specimen, within 48 h a substantial amount of the nickelocene has migrated through the atmosphere and is adsorbed in the pores of the silica (Figure 2). When the distance between the

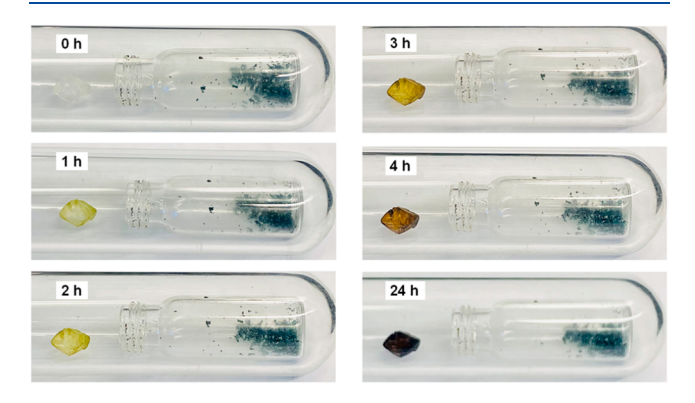


Figure 2. Nickelocene migrating to a silica specimen through the inert gas atmosphere and adsorbing on the surface within its pores.

vial and the silica piece is increased, the colorful nickelocene takes longer to migrate (Figure S2). Overall, the process is complete within 2 days.

The pure polycrystalline 1 is rather stable and remains green throughout the experiment (Figure 2). It can be washed off completely with THF (Figure S1). However, when 1 is adsorbed on the silica surface it is much more vulnerable, and traces of oxygen transform it into a nickel oxide hydroxide species (Figure S2). This oxidized form that is brown/black depending on the concentration (Figure S2) remains firmly bound to the surface and cannot be washed off with an organic solvent

The samples studied by solid-state NMR have been prepared by adsorption of 1 on a silica surface with different loadings. Surface coverages of 70%, 140%, and 200% have been obtained by gentle dry grinding of 1 with the corresponding amounts of silica. For simplicity, the samples will be denoted as 1-70, 1-

140, and 1-200 in the following. The targeted surface coverages have been determined as described earlier for ferrocene.²¹ For comparison, a sample containing ferrocene (2) adsorbed on the silica surface with a 70% coverage has also been prepared (2-70).

 1 H and 13 C solid-state NMR spectra have been recorded at different temperatures. These studies included 1 H T_{1} relaxation time measurements performed by inversion recovery experiments. Unfortunately, as demonstrated above, 1 is not stable on the silica surface over prolonged periods of time at room temperature. A broad 1 H resonance at about 5 ppm appears in the 1 H NMR spectra of static samples, which is growing over 24 h. This signal most probably belongs to a decomposition product, such as cyclopentadiene or its Diels—Alder addition product dicyclopentadiene. Nevertheless, by use of freshly prepared samples, mostly the signals of adsorbed, but not chemically reacted, nickelocene are visible in the spectra.

As outlined above, nickelocene is paramagnetic, with an electron spin S = 1, and therefore its ${}^{13}C$ and ${}^{1}H$ MAS NMR spectra display paramagnetic, large 13C and 1H chemical shift values that are mainly caused by Fermi contact electron-nucleus interactions.^{29,31–33,38,39} Because of the Fermi contact contributions, the isotropic 13C resonance of the cyclopentadienyl (C₅H₅, Cp) rings in 1 is observed at a very low magnetic field with an isotropic chemical shift $\delta_{\rm iso}(^{13}{\rm C})$ of 1594–1579 ppm²⁹ or 1514³⁹ ppm. The isotropic ¹H resonance is shifted toward high field and shows a $\delta_{iso}(^{1}H)$ value of -257ppm (Figure 1, top).²⁹ The exact δ_{iso} of both nuclei in 1 and also their CSA values strongly depend on the measurement temperature, ^{29,32,38} again due to Fermi contact interactions. Therewith, the chemical shift and CSA values also depend indirectly on the MAS speed because due to friction the rotors heat up at higher rotational frequencies.³⁰ In addition, anisotropic interactions, such as spin dipolar interactions, dipolar diamagnetic interactions, and bulk magnetic susceptibility (BMS) effects, result in large chemical shift anisotropies. They can reach, for example, 2600 ppm in the case of the ¹³C nuclei in 1,²⁹ complicating their experimental detection.

In accordance with the above-mentioned literature, the $^1\mathrm{H}$ MAS NMR spectrum of polycrystalline 1 (Figure 3, top), used as a reference, exhibits a spinning sideband pattern with a proton isotropic chemical shift $\delta_{\mathrm{iso}}(^1\mathrm{H})$ of -248 ppm. Interestingly, the distribution of the spinning sideband intensities in this manifold is very close to that observed for vanadocene. 32

Because the MAS NMR experiments have been applied in this contribution only for qualitative considerations, we did not make temperature corrections to account for the heating of the samples at high spinning rates (see above).30 Inversion recovery experiments, performed for polycrystalline 1 at 295 K, yielded different relaxation times for the sidebands and the isotropic resonance in the partially relaxed ¹H MAS NMR spectra. The ${}^{1}H$ T_{1} time amounts to 0.28 ms for the isotropic resonance and equals 0.25 and 0.21 ms for the first-order downfield and upfield sidebands, respectively. This result, revealing the presence of a ${}^{1}H$ T_{1} time distribution in 1, is often observed for paramagnetic systems.³¹ Naturally, it complicates the interpretation of T_1 time data. Nevertheless, the measured ${}^{1}H$ T_{1} times are all very short, in agreement with the assumption that the Fermi-contact interactions are dominant. The latter lead to a scenario where the relaxation of the nuclei depends on the electron relaxation and is independent from molecular dynamics. It is remarkable that

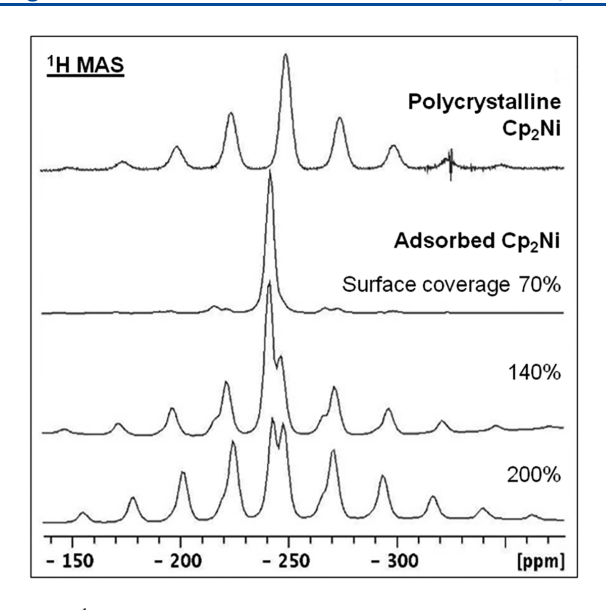


Figure 3. ¹H MAS NMR spectra of polycrystalline and adsorbed 1, recorded at 295 K with a spinning rate of 10 kHz. From top to bottom: compound 1 and materials 1-70, 1-140, and 1-200.

the line width $\Delta\nu$ of the Cp resonance in the 1H MAS NMR spectrum of 1 (Figure 3, top), which equals 2.5 kHz at 295 K, gives a 1H T_2 time of 0.12 ms (or 0.40 ms) for a Lorentz (or Gauss) resonance shape, in agreement with the above 1H T_1 time. The $\Delta\nu$ value of the Cp resonance changes with the temperature from 3.5 kHz at 283 K to 4.0 kHz (273 K), 4.8 kHz (263 K), and 5.5 kHz (253 K) (Table 1). This feature will be used below for quantitative estimates based on a line shape analysis.

Table 1. Line Widths $\Delta \nu$ in the Static ¹H NMR Spectra of Polycrystalline 1 and Adsorbed 1-70 Measured in kHz at Different Temperatures^a

T (K)	1 Δu $(\Delta u_{ m rot})$ $({ m kHz})$	1-70 $\Delta \nu$ (kHz)
295	41.6 (2.5)	8.4
283	44.9 (3.5)	11.6
273	49.6 (4.0)	18.7
263	50.7 (4.8)	22.4
253	53.6 (5.5)	30.9
245	54.4	46.8
235	55.9	58.9
225	64	79.5
205	68	94.5
185	73.6	116
175		140

 a The line widths $\Delta \nu_{\rm rot}$ in the 1 H MAS NMR spectra of 1, spinning at 10 kHz, are given in parentheses for accessible temperatures.

One section of the temperature-dependent ¹H NMR spectra of a static sample of **1** is shown in Figure 4. The ¹H background signal from the probehead between 0 and 10 ppm has been subtracted for clarity. As Figure 4 shows, upon cooling, the ¹H resonance of **1** experiences a strong upfield shift. The corresponding values are graphically displayed in Figure 5. This behavior is well documented for nickelocene and vanadocene. ^{29,38}

The observed chemical shift change is accompanied by a moderate increase in the line widths $\Delta \nu$, which are

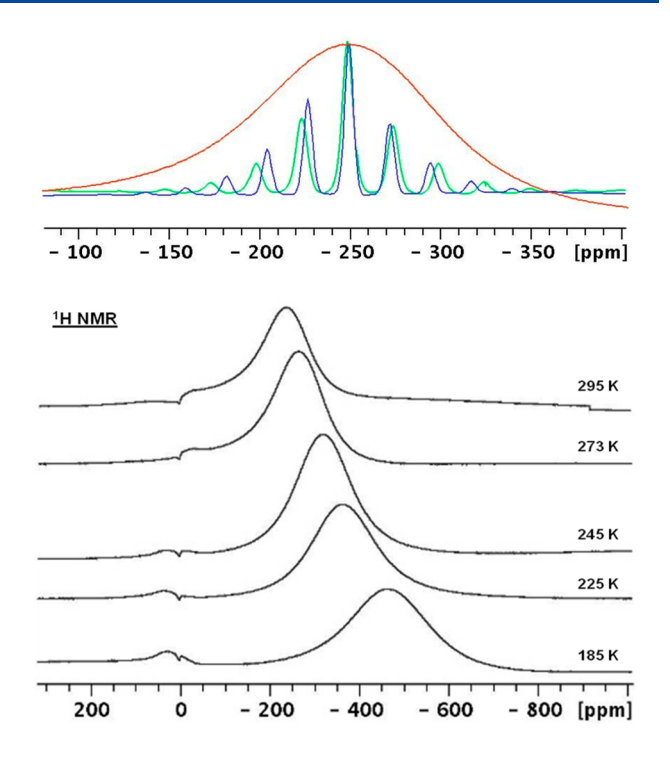


Figure 4. VT 1 H wide-line NMR spectra of polycrystalline 1 at the indicated temperatures. The display on the top shows the static 1 H (brown, 295 K) and MAS NMR spectra of 1 spinning at 10 kHz (green) and 9 kHz (blue).

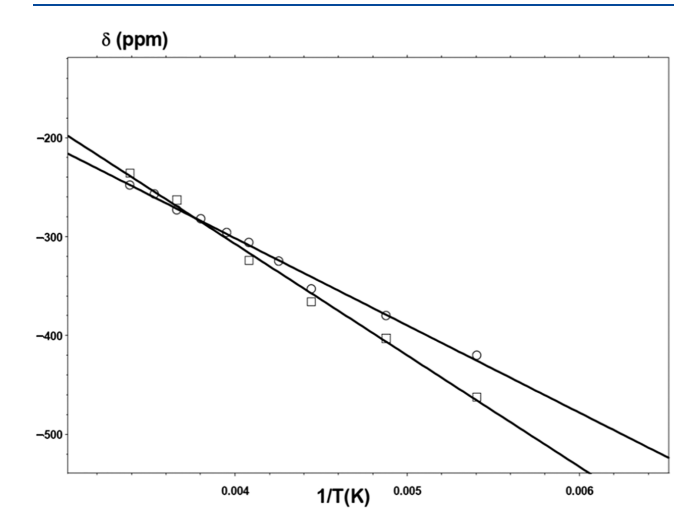


Figure 5. Temperature dependence of the ¹H Cp chemical shifts in the NMR spectra of static samples of polycrystalline 1 (\square) and 1-70 (\bigcirc), presented in coordinates of δ versus 1/T.

summarized in Table 1 and graphically displayed in Figure 6. Correspondingly, as the temperature is lowered, the ¹H CSA values are increasing (Table 2). Both effects, as mentioned above, are already known for 1.²⁹ However, in this study, we will use these parameters to characterize compound 1 as a reference for an immobile molecule. Hereby, the exceptionally fast rotation of the Cp rings^{30,40} is not considered.

In general, the analysis of the sideband patterns in the ¹H MAS NMR spectra of polycrystalline 1 (Figure 3, top) to determine the ¹H CSA values is not trivial. The reason for this is that in solid materials the shift anisotropies are governed by the spin dipolar interactions, diamagnetic dipolar interactions

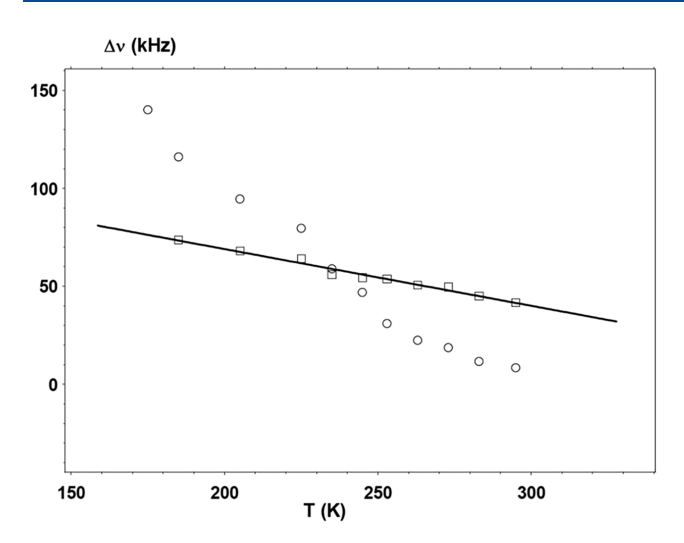


Figure 6. Correlation of the line widths $\Delta \nu$ with the temperature for polycrystalline 1 (\square) and adsorbed 1-70 (\bigcirc).

Table 2. Chemical Shift Anisotropy Parameters, 1 H CSA, and Asymmetry Parameter, η , Obtained by a Sideband Analysis Performed for 1 H MAS NMR Spectra of 1 Spinning at a Rate of 10 kHz in the Temperature Range between 305 and 263 K

T (K)	¹ H CSA (ppm)	η
305	52	0.86
295	55.5	0.89
283	57	0.95
273	61	0.90
263	66	0.80

(proton–proton), and BMS effects, sometimes in the presence of large contact interactions. This combination of interactions obviously leads to distorted intensities in spinning sideband manifolds. In fact, the $^1{\rm H}$ MAS NMR spectrum of polycrystalline 1 cannot be simulated as a single CSA pattern. However, it can be reproduced by using at least two sets of sideband patterns with a $^1{\rm H}$ CSA of 56 ppm and an asymmetry parameter $\eta=0.9$ (the high-intensity manifold) and a $^1{\rm H}$ CSA of 127 ppm and $\eta=0.9$ (the low-intensity manifold) (Figure S3). It should be emphasized that this approach does not represent the actual situation. It illustrates, however, a poor simulation of the low-intensity sidebands when using only the first set of parameters.

Unfortunately, the experimental ¹H CSA values for Cp rings in metallocenes are not available. First-principles calculations using relativistic approximations have resulted in a scenario where the CSA of 1 is dependent on the calculation levels: around 105–108 or 64–67 ppm. ⁴¹ It is remarkable that the ¹H CSA of 64–67 ppm corresponds to the value obtained experimentally at 263 K (Table 2). However, the theoretical calculations ⁴¹ were performed by assuming an axially symmetric chemical shift tensor while the experimental sideband manifolds displayed in Figure 4 and Figure S3 do not have this symmetry. The latter is also valid for the ¹H MAS NMR of vanadocene. ³² Given this complex situation, in the following we use the CSA of the major component (Table 2) for the interpretation of the temperature-dependent ¹H line shapes in the spectra of polycrystalline 1 and adsorbed 1-70.

As follows from Figure 3, the ^1H MAS NMR spectrum of material 1-70 manifests a resonance at $\delta_{\rm iso}$ of -243 ppm with very low-intensity sidebands. These sidebands disappear completely in the temperature range from 315 to 325 K. Thus, in a submonolayer coverage, compound 1 behaves like a liquid on the silica surface. In full accordance with this behavior, the ^{13}C MAS NMR spectrum of 1-70 recorded at 325 K (Figure 7) shows a resonance at 1415 ppm, corresponding to $\delta_{\rm iso}(^{13}\text{C}),^{29}$ which is not accompanied by spinning sidebands.

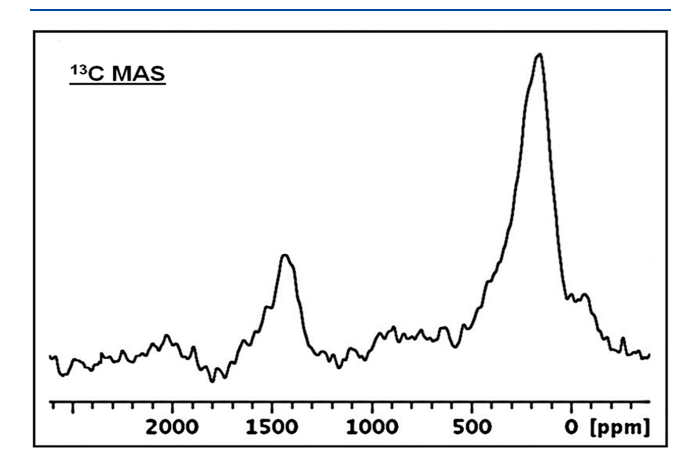


Figure 7. ¹³C MAS NMR spectrum recorded at 325 K for a sample of 1-70, spinning at a rate of 9 kHz. The high-field resonance corresponds to the decomposition product that appears during prolonged accumulation.

To characterize the molecular dynamics of the adsorbed nickelocene in 1-70, we applied the static ¹H NMR experiments that require no temperature corrections, in contrast to MAS NMR.³⁰ Selected ¹H wide-line spectra are displayed in Figure 8.

The wide-line spectra clearly show a temperature evolution of the ^1H NMR resonance from a liquidlike signal to a very broad line with a line width $\Delta\nu$ reaching about 140 kHz at 175 K (Table 1). Note that the ^1H T_1 time of the liquidlike signal of 1-70 (0.56 ms) is slightly longer than in polycrystalline 1.

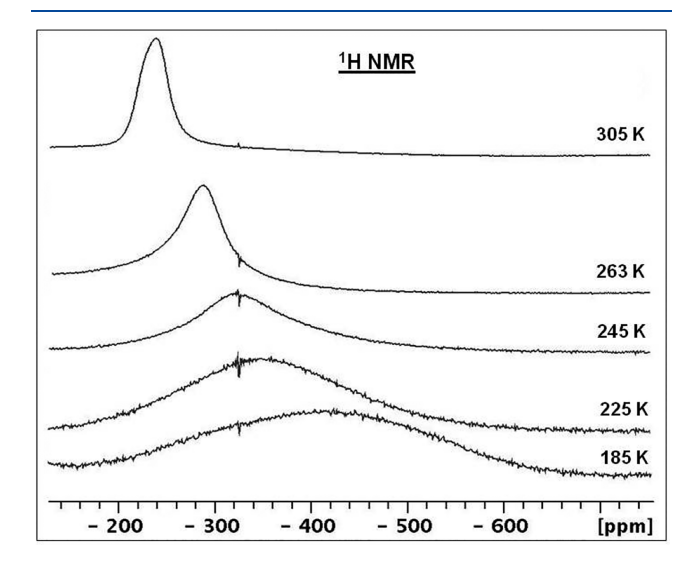
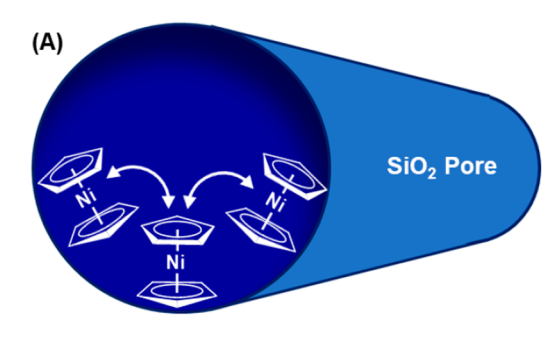


Figure 8. Selected variable temperature ¹H wide-line NMR spectra of 1-70 obtained without sample rotation at the indicated temperatures.

This is probably due to the appearance of a relaxation contribution that is dependent on molecular correlation times.³³ Comparison of the $\Delta \nu$ parameters, presented for 1 and 1-70 in Table 1 and Figure 6, reveals that below 225 K the line widths of the signals of 1-70 become substantially larger than for 1, showing a big difference of 42 kHz at 185 K. A formal calculation gives the ¹H CSA values of 111 and 162 ppm for 1 and 1-70, respectively. Because C5 rotations of the Cp rings in polycrystalline 1, as well as in neat ferrocene, 23 are very fast^{30,40} and can be detected by NMR only at 110 K, we explain the observed difference by retardation of the Cp rotations in nickelocene molecules that are located horizontally on the silica surface. In case the metallocenes were "standing upright" with the Cp rings parallel to the surface, at least one of the Cp rings would display unhindered rotation. In this case, two signals would have been expected in the low-temperature spectra shown in Figure 8. Note that the horizontally oriented states of the ferrocene on the silica surface, with the Cp rings perpendicular to the surface, were found as the most stable ones in earlier research.²³ It is quite probable that molecule surface interactions are stronger in the case of adsorbed nickelocene in sample 1-70, causing the retardation at the lowest temperatures mentioned above. In comparison, the most stable state of benzene adsorbed on activated carbon⁴ or SBA-15⁴² is an orientation parallel to the surface. Obviously, the metal and the changed overall geometry have an impact on the preferred orientation of the metallocenes. The behavior of a potential "missing link" between benzene and metallocenes, adsorbed (C₆H₆)₂Cr, will be investigated by VT solid-state NMR in a future project.

By analogy with ferrocene (2) adsorbed in a submonolayer on the silica surface, ²³ the temperature evolution of the ¹H resonance in Figure 8 can correspond to two possible motional mechanisms (Figure 9). (A) Consistent motions of the



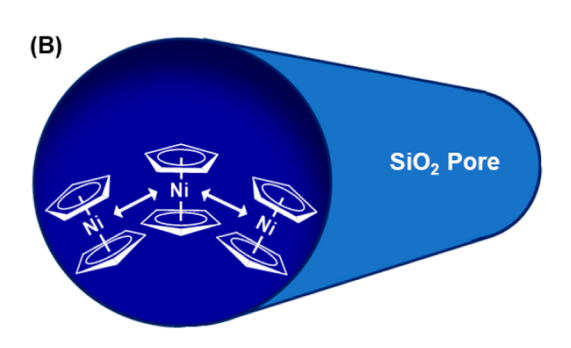


Figure 9. Two motional models A and B that can explain the sharp proton resonance of nickelocene on the silica surface.

adsorbed molecules along the surface (a "tumbleweed scenario", situation A in Figure 9), ¹⁹ which imitate isotropic reorientations without detachment from the surface, could occur. (B) Alternatively, a chemical exchange on the NMR time scale between liquidlike, surface-detached, truly isotropically moving states and adsorbed immobile molecules (situation B in Figure 9) could take place. The expected spectral feature of situation B is a coexistence of the isotropic (sharp) and immobile (broad) resonances in the variable temperature NMR spectra, as it was earlier observed for ferrocene by ¹³C and ²H NMR. ²³ To verify this feature for 2 with ¹H NMR, the VT spectra were recorded for sample 2-70 (Figure 10). As can clearly be seen in Figure 10 and the

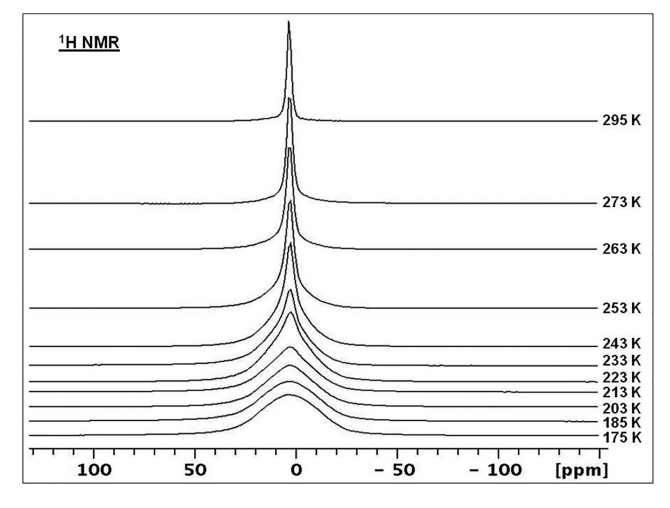


Figure 10. Variable temperature ¹H wide-line NMR spectra obtained for a static sample of adsorbed ferrocene **2-70** at the indicated temperatures.

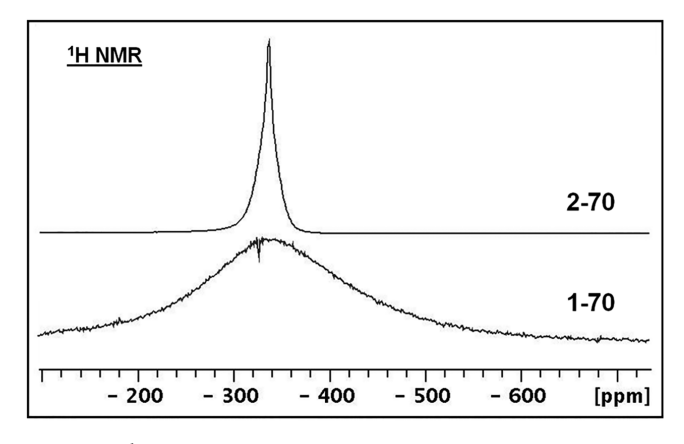


Figure 11. ¹H wide-line NMR spectra of adsorbed ferrocene 2-70 and nickelocene 1-70 recorded at 235 K without sample rotation. The resonance of 2-70 is displayed on top of the resonance of 1-70 for comparison. The chemical shift scale only accounts for 1-70.

comparison of signals of 2-70 and 1-70 in Figure 11, the spectra of adsorbed ferrocene show this coexistence in contrast to the spectra of 1-70. Therefore, model B with the truly isotropically moving states can be ruled out for adsorbed nickelocene. It should be noted, however, that model B can also be realized if the isotropically moving species are

intermediates which are not visible in NMR. Under these conditions models B and A would be topologically different but spectroscopically identical.

Finally, as follows from Figure 12, increasing the surface coverage leads to a remarkable decrease in the transformation

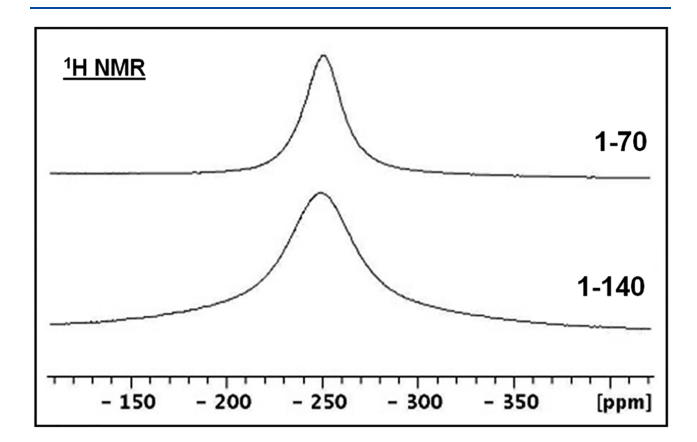


Figure 12. ¹H wide-line NMR spectra of materials 1-70 (top) and 1-140 (bottom) recorded at 295 K without sample rotation.

rate of anisotropic molecular to liquidlike states due to a decrease of the number of free surface sites. Spectroscopically, this corresponds to the strong broadening of the ¹H resonance in 1-140.

The kinetic parameters of the process evolving on the silica surface can in principle be obtained by quantitative treatments of the VT ¹H NMR spectra (Figure 8), where a line shape analysis plays the central role. However, because of the variety of contributions to the shape of the ¹H static signal (anisotropic spin dipolar interactions, proton-proton dipolar interactions, and BMS anisotropy⁷) and the impossibility of their accurate separation, such an analysis becomes problematic. In this context, additional information is needed, which can be obtained by considering the ¹H MAS NMR spectra in Figure 3, where material 1-70 is compared with 1-140 and 1-200, containing an excess of 1. As these ¹H MAS NMR spectra show, in contrast to polycrystalline 1 and sample 1-70, the materials 1-140 and 1-200 exhibit two sets of signals at $\delta_{\rm iso}(^{1}{\rm H}) = -243$ and -247 ppm. In both cases, the resonance at -243 ppm, accompanied by spinning sidebands with lower intensities, belongs to more mobile molecules of 1. The general observation that at a higher loading two phases are formed, a mobile surface phase and a stationary bulk phase, is most common when there are no particularly strong interactions between the guest molecules. 43 It is interesting that the ratio of less mobile to more mobile molecules is determined to be 1.3 to 1 and 3.5 to 1 for 1-140 and 1-200, respectively. Again, lower mobility is found for increased surface coverages, as communicated earlier for adsorbed 2. 20-22 In addition, there is no exchange between less mobile and more mobile states. This situation can be realized assuming the presence of inhomogeneous distribution of the molecules among silica pores of different sizes or limited contact of the remaining polycrystalline with adsorbed nickelocene. Alternatively, in contrast to 2,²¹ the stronger adsorption of 1 might prevent rapid exchange between adsorbed and polycrystalline nickelocene on the surface.

The formal sideband analysis of the signals in Figure 3, performed within the limits of the ¹H CSA, resulted in the

following anisotropy parameters: CSA = 56 ppm at η = 0.9 for compound 1; CSA = 16 ppm at η = 0.95 for material 1-70; CSA = 32 ppm at $\eta = 0.8$ (-243 ppm) and CSA = 65 ppm at η = 0.95 (-247 ppm) for material 1-140; CSA = 35 ppm at η = 0.9 (-243 ppm) and CSA = 62 ppm at η = 0.9 (-247 ppm) for material 1-200. As one can see, at room temperature the materials 1-140 and 1-200 contain immobile nickelocene molecules with CSA values that are close to those of polycrystalline 1. Additionally, there are mobile molecules with ¹H CSA values increasing from 16 ppm (1-70) over 32 ppm (1-140) to 35 ppm (1-200). Thus, this effect illustrates a retardation of the observed motional process by decreasing the number of unoccupied surface sites. This allows us to analyze the VT ¹H NMR spectra of 1-70 or 1-140 by observing the loss of the CSA with increasing the temperature. Note that the temperature-dependent CSA parameters of polycrystalline 1 (Table 2) can be applied as a reference for the immobile compound in the following calculations performed for 1-70.

Figure 13A displays the static ¹H NMR spectrum of 1 at 295 K, accompanied by a static line shape. This shape was

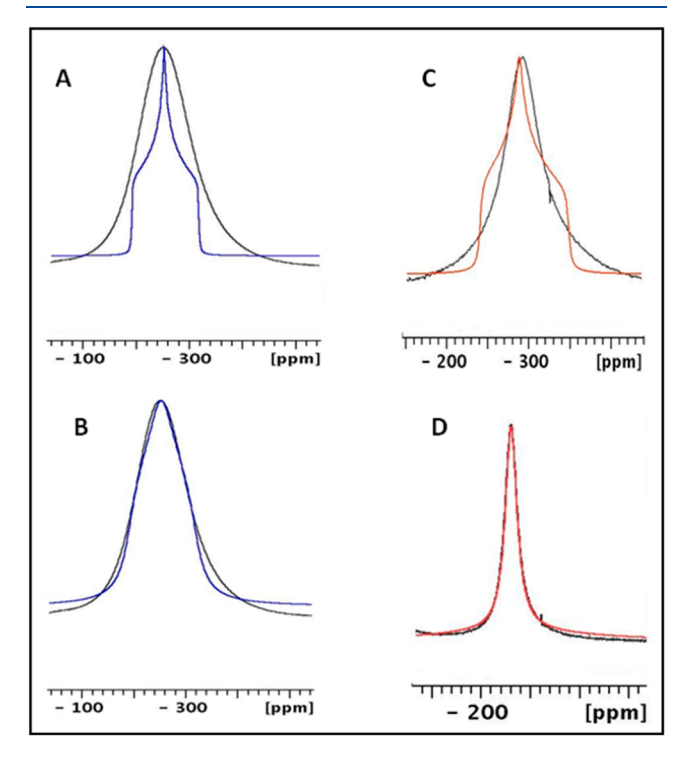


Figure 13. (A) Static ¹H NMR spectrum of 1 at 295 K (black) and the line shape (blue), calculated with the CSA parameters of 1 on the basis of its ¹H MAS NMR spectrum providing the natural line width. (B) Line shape of 1 as in (A), calculated after addition of 10–12 kHz line broadening to the natural line width, caused by proton—proton dipolar interactions present in the static sample. (C) Static ¹H NMR spectrum of 1-70 at 263 K (black) and the line shape (brown) calculated for 1 based on the CSA in Table 2 where the calculated singularities were applied for an analysis of three-centered exchange (see text). (D) Best fitting obtained for the ¹H NMR spectrum of 1-70 at 283 K within the limits of the three-centered exchange.

calculated with the CSA parameters summarized in Table 1, including $\Delta\nu_{\rm rot}$ as the characteristics of a natural line width. Obviously, both line shapes differ substantially. However, the situation changes remarkably when 10–12 kHz are added to the natural line width (Figure 13B). This magnitude

representing typical proton—proton dipolar contributions was estimated from the broad component in the low-temperature ¹H NMR spectra of the diamagnetic adsorbed ferrocene in sample 2-70 (Figure 11).

Table 1 shows that at temperatures higher than 245 K the $\Delta \nu$ values in 1-70 are more than 10 kHz smaller than in 1. Hence, if the rate of molecular motions in 1-70 is faster than 1 \times 10⁴ s⁻¹, the dipolar proton-proton contribution will be negligible. In other words, quantitative treatments of the ¹H NMR spectra of 1-70 are simplified, and they can be performed on the basis of the CSA alone. Such a situation is shown in Figure 13C, where the ¹H static NMR spectrum of 1-70 at 263 K is compared with the line shape calculated for 1 on the basis of the CSA in Table 2. Consequently, the singularities in this shape, corresponding to the chemical shifts δ_{11} , δ_{22} , and δ_{33} , can be used within the limits of a three-centered exchange (see, for example, Figure 13D) to determine the rate (k) of the loss of the CSA due to motions of 1 on the silica surface. These calculations were performed by using the temperaturedependent $\Delta \nu_{\rm rot}$ values for 1 (Table 1) as the natural line widths and at the constant line width of 7.2 kHz observed for 1-70 at 325 K. The resulting k values were averaged and are summarized in Table 3.

Table 3. Temperature Dependence of the Rate Constants k (s⁻¹) Obtained by Analysis of the Static ¹H NMR Spectra of Material 1-70 (See Text)

T (K)	$k (10^{-3} \text{ s}^{-1})$
295	830/439 ^a
283	582
273	450/219 ^a
263	341
253	217
245	177
4-1	

^aObtained for material 1-140.

First of all, the obtained data show that when going from 1-70 to 1-140 the motional rate k decreases by approximately a factor of 2. Second, the temperature dependencies of the rate k in coordinates of $\ln(k)$ versus 1/T (Figure 14) or $\ln(k/T)$

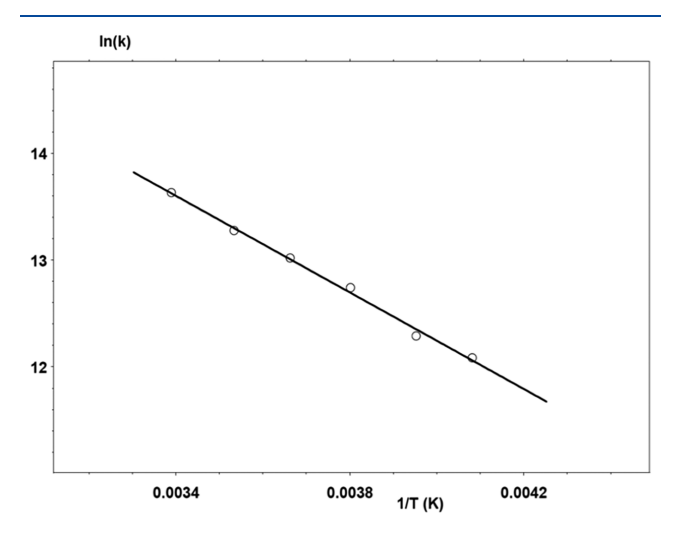


Figure 14. Temperature dependence of the rate constants k obtained for 1 adsorbed on the silica surface in a submonolayer (sample 1-70) in coordinates of $\ln(k)$ versus 1/T.

versus 1/T (Figure 15) form ideal straight lines that allow the determination of the kinetic parameters $E_{\rm act} = 5.5$ kcal/mol, $A = 1.1 \times 10^{10}$, $\Delta H^{\ddagger} = 5.0$ kcal/mol, and $\Delta S^{\ddagger} = -15$ eu.

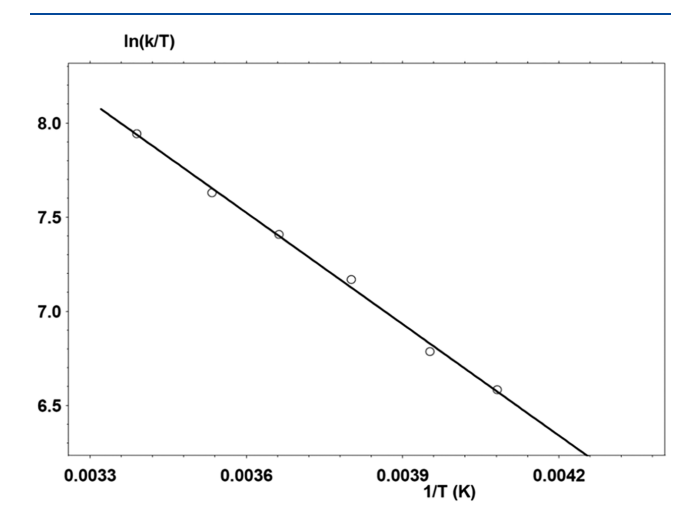
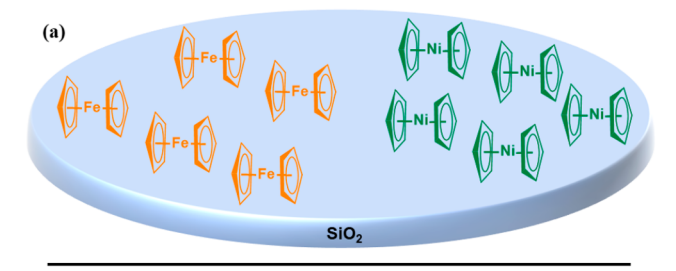


Figure 15. Temperature dependence of the rate constants k obtained for material 1-70 in coordinates of $\ln(k/T)$ versus 1/T.

Next, we investigated whether metallocene molecules mix on the surface on the molecular level or whether they occupy different domains on the surface in the form of patches (Figure 16). This is an important question with respect to forming dual



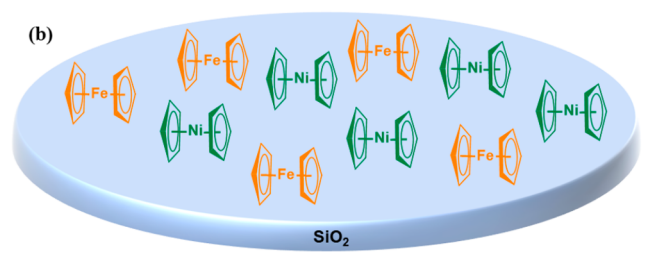


Figure 16. Mixing of ferrocene and nickelocene on the silica surface in submonolayer amounts could result in patches (a) or homogeneous mixing on the molecular level (b).

atom catalysts from different metallocenes spread out on the silica surface. For this investigation, we mixed systems containing paramagnetic 1 and diamagnetic 2 in the material 1-40-2-40 (40% for each component to account for a total surface coverage of 80%).

The room temperature 1 H NMR spectra of **1-40-2-40**, recorded in static and spinning regimes are shown in Figure 17. Two isotropic resonances in a 1:1 ratio are observed at 5.1 and -250.6 ppm for compounds **2** and **1**, respectively. The 1 H T_{1} times of the signals determined in spinning and static samples by inversion recovery experiments performed at two carrier

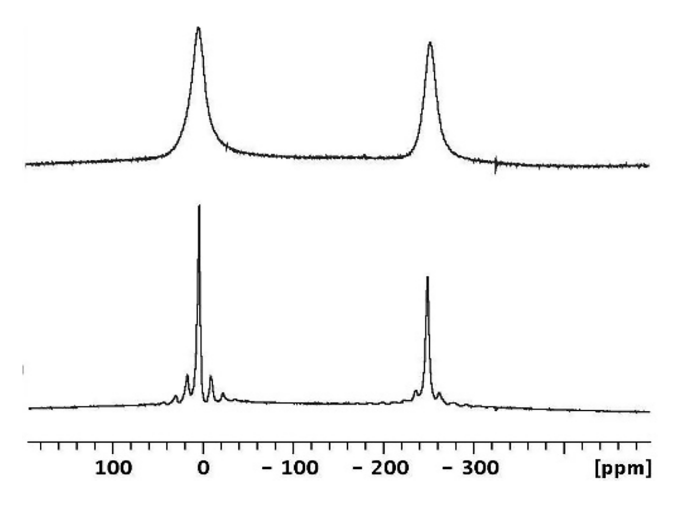


Figure 17. ¹H solid-state NMR spectra of material 1-40-2-40 recorded at 295 K in the static (top) and spinning (5 kHz) regime (bottom).

frequencies centered at positions of both resonances are summarized in Table 4. The very short ${}^{1}H$ T_{1} time of

Table 4. 1 H T_{1} Relaxation Times (ms) Measured for Compounds 1 and 2 in Static (St) and Spinning (Sp) Material 1-40-2-40

		1		2
T (K)	T_1 (st)	T_1 (sp) (kHz)	T_1 (st)	T_1 (sp) (kHz)
305	0.43	0.44 (8)	12	12.6 (8)
295	0.45	0.42 (5)	9.8	14.0 (5)
283	0.36	0.35 (5)	9.1	14.0 (5), 16.8 (8)
273	0.35		8.4	
263			7.0	
253	0.32			
243	0.35			
223	0.42			

paramagnetic 1 in the material 1-40-2-40 does not depend on the spinning rate or on the temperature, in agreement with the dominance of the Fermi contact relaxation mechanism for the Cp protons of 1. 31,33 The 1 H T_{1} time of 1 in 1-40-2-40 is also in the same range as determined for adsorbed nickelocene 1-70 (0.56 ms).

The 1 H T_1 time of diamagnetic, polycrystalline ferrocene 2 amounts to 14.0 s (5 kHz). When compound 2 is adsorbed on silica with surface coverages of 40% and 80%, the 1 H T_1 relaxation times for the static samples are reduced to 0.24 and 0.53 s, respectively. In comparison, the 1 H T_1 values for surface-adsorbed 2 in the mixture with adsorbed paramagnetic 1 in sample 1-40-2-40 are orders of magnitude smaller (Table 4). As compared to the adsorbed component 1, however, these values are substantially longer, slightly diminished upon cooling, and dependent on the spinning rate. The dependence of T_1 on the spinning speed is indicative of the spin diffusion relaxation mechanism, 31,33 which is effective for the diamagnetic compound 2.

The obtained data for adsorbed 2 versus 2 in combination with adsorbed nickelocene show that molecules of 1 and 2 are neighboring in the pores of 1-40-2-40, where they are mixing on the molecular level. The spin-diffusion effective for compound 2 is caused by strong proton—proton dipolar

coupling between these molecules. It is remarkable that the spin-diffusion relaxation is effective for protons of **2** in spite of the relatively narrow signals in the $^1\mathrm{H}$ NMR spectra in Figure 17 showing molecular reorientations of both components. In principle, the further investigation of the spin diffusion itself as performed, for example, to study the compatibility of solid polymer blends 44 would be interesting. However, the measurements of $T_{1\rho}$ relaxation times and especially their quantitative interpretation would be complicated by the presence of the paramagnetic nickelocene. Additionally, the T_1 dependence on the spinning rates is not strong (Table 4) and thus does not affect the main conclusion that ferrocene and nickelocene adsorbed in a submonolayer on silica form a homogeneous mixture.

CONCLUSION

The results described in this contribution show that nickelocene can be adsorbed on a silica surface by combining the two solids or by adsorption from the gas phase at ambient temperature. Visualization experiments on the macroscopic scale allow to establish a timeline for the adsorption process. It has been demonstrated that a well-defined monolayer of nickelocene molecules forms on the surface. Although a solidsolid interface is present, nickelocene shows different modes of mobility on the surface. Paramagnetic solid-state NMR spectroscopy has been employed to describe the dynamics of the adsorbed nickelocene molecules. ¹³C and ¹H VT wide-line and MAS spectra as well as CSA evaluations lead to the conclusion that besides the translational mobility of nickelocene, an isotropic reorientation takes place on the surface (model A, Figure 9). This reorientation can be described as a tumbleweed motion where the molecules stay attached to the surface. The states of the surface-attached horizontally oriented nickelocene molecules have been quantified. The temperature dependencies of the rate k in coordinates of ln(k) versus 1/Tand ln(k/T) versus 1/T form ideal straight lines that allow the determination of the kinetic parameters $E_{act} = 5.5$ kcal/mol, A = 1.1 × 10¹⁰, ΔH^{\ddagger} = 5.0 kcal/mol, and ΔS^{\ddagger} = -15 eu. Interestingly, the observed surface-molecule interactions of nickelocene are very different from those of ferrocene adsorbed on silica,²³ where temporary detachment of the molecules from the surface takes place (model B, Figure 9), leading to randomly changed orientation of the rotational axis. It is remarkable that the latter is often considered as interpretation of the molecular dynamics in highly viscous liquids that are investigated theoretically and experimentally by dielectric spectroscopy and NMR spectroscopy, including NMR relaxation. 45-48 We will investigate this aspect in future research.

Finally, it has been demonstrated by T_1 relaxation time measurements that nickelocene and ferrocene molecules adsorbed on the same silica surface in submonolayer amounts are mixing on the molecular level. While the formation of a well-defined monolayer of nickelocene on the silica surface is crucial for the formation of Ni SACs, the mixed nickelocene and ferrocene molecules might allow the formation of dual atom catalysts in the future.

■ EXPERIMENTAL SECTION

Materials. The silica (Merck, 40 Å average pore diameter, 0.063-0.2 mm average particle size, specific surface area 750 m²/g) was dried in vacuo at 200 °C for 2 days to remove adsorbed water and condense surface silanol groups⁴⁹ and stored under an inert atmosphere.

Sample Preparation. All materials were handled, stored, and filled into the rotors under an inert atmosphere. The maximal surface coverage of the silica with **2** has been determined earlier. Because ferrocene and nickelocene have the same foot prints, samples of adsorbed **1** can be prepared by using the same molar amounts. Sample **1-70** was prepared by gentle dry grinding of 191.0 mg (1.011 mmol) of Cp_2Ni (1) with 256 mg of silica in a glovebox for 1.5 min by using a pestle and mortar. Sample **1-140** was created by dry grinding of 1 (188.0 mg, 0.995 mmol) with 127 mg of silica. The sample **1-200** was prepared by dry grinding of 277.0 mg (1.467 mmol) of **1** with 126 mg of silica. All measured samples of **1** adsorbed on silica displayed a moss green color. For sample **1-40-2-40** 0.500 g of silica was mixed together with 0.113 g (0.607 mmol) of Cp_2Fe (2) and 0.116 g (0.614 mmol) of **1** in a glovebox.

NMR Instrumentation and Measurements. The ¹³C{¹H} and ¹H MAS and static ¹H NMR experiments were performed with a Bruker Avance 400 solid-state NMR spectrometer (400 MHz for ¹H nuclei) equipped with a two-channel 4 mm MAS probe head. The standard single-pulse sequences (direct nuclear excitation with a 50° radio frequency (RF) pulse) were applied for the ¹³C nuclei by using recycle delays as needed for the corresponding full spin–lattice relaxation estimated based on the inversion–recovery experiments.

The static ¹H NMR data were collected with a solid-echo pulse sequence $(90^{\circ}-\tau-90^{\circ})$ with a τ delay of 40 μ s, a 90° pulse length of 5.25 μ s, and a relaxation delay of 4 s.

All samples were densely packed into the insert-free rotors as finely ground powders. Compressed nitrogen was used as both the bearing and drive gas for the MAS measurements.

The variable-temperature $^{13}\mathrm{C}$ and $^{1}\mathrm{H}$ NMR experiments have been performed with a standard temperature unit of the spectrometer calibrated with liquid methanol placed into a 4 mm rotor. The experimental $^{13}\mathrm{C}$ and $^{1}\mathrm{H}$ T_1 relaxation times were measured by inversion—recovery (180° $-\tau$ –90°) experiments, and RF pulses were calibrated and τ delays widely varied to determine rough T_1 estimates. Pulse delays were adjusted to provide full nuclear relaxation in each cycle.

The experimental 1 H inversion—recovery data for the displays of signal intensity versus τ time have been treated with a standard nonlinear fitting computer program based on the Levenberg—Marquardt algorithm. 50 The statistical errors of the 1 H T_1 time determinations were <15%. The line shape analysis of the static 1 H VT NMR spectra was performed with the program DNMR in the software package of the Bruker spectrometer.

ASSOCIATED CONTENT

5 Supporting Information

The Supporting Information is available free of charge at https://pubs.acs.org/doi/10.1021/acs.langmuir.2c00301.

Removal of adsorbed nickelocene from silica by washing (Figure S1), migration of nickelocene through space and adsorption on silica (Figure S2), and simulation of the ¹H MAS NMR spectrum of nickelocene (Figure S3) (PDF)

AUTHOR INFORMATION

Corresponding Authors

Janet Blümel – Department of Chemistry, Texas A&M University, College Station, Texas 77845-3012, United States; o orcid.org/0000-0002-6557-3518;

Email: bluemel@tamu.edu

Vladimir I. Bakhmutov — Department of Chemistry, Texas A&M University, College Station, Texas 77845-3012, United States; Email: bakhmoutov@chem.tamu.edu

Authors

Jordon W. Benzie – Department of Chemistry, Texas A&M University, College Station, Texas 77845-3012, United States

Gabrielle E. Harmon-Welch – Department of Chemistry, Texas A&M University, College Station, Texas 77845-3012, United States

John C. Hoefler – Department of Chemistry, Texas A&M University, College Station, Texas 77845-3012, United States

Complete contact information is available at: https://pubs.acs.org/10.1021/acs.langmuir.2c00301

Notes

The authors declare no competing financial interest.

ACKNOWLEDGMENTS

This work was supported by the National Science Foundation (CHE-1900100).

REFERENCES

- (1) Shenderovich, I. G.; Limbach, H.-H. Solid State NMR for Nonexperts: An Overview of Simple but General Practical Methods. *Solids* **2021**, *2*, 139–154.
- (2) Duncan, T. M. A Compilation of Chemical Shift Anisotropies; Farragut Press: Chicago, IL, 1990.
- (3) Guenther, J.; Reibenspies, J.; Blümel, J. Synthesis and characterization of tridentate phosphine ligands incorporating long methylene chains and ethoxysilane groups for immobilizing molecular rhodium catalysts. *Mol. Catal.* **2019**, *479*, 110629.
- (4) Benzie, J. W.; Bakhmutov, V. I.; Blümel, J. Benzene Adsorbed on Activated Carbon: A Comprehensive Solid-State NMR Study of Interactions with the Pore Surface and Molecular Motions. *J. Phys. Chem. C* **2020**, *124*, 21532–21537.
- (5) Hilliard, C. R.; Kharel, S.; Cluff, K. J.; Bhuvanesh, N.; Gladysz, J. A.; Blümel, J. Structures and Unexpected Dynamic Properties of Phosphine Oxides Adsorbed on Silica Surfaces. *Chem.—Eur. J.* **2014**, 20, 17292–17295.
- (6) Kharel, S.; Cluff, K. J.; Bhuvanesh, N.; Gladysz, J. A.; Blümel, J. Structures and Dynamics of Secondary and Tertiary Alkylphosphine Oxides Adsorbed on Silica. *Chem.—Asian J.* **2019**, *14*, 2704–2711.
- (7) Hubbard, P. J.; Benzie, J. W.; Bakhmutov, V. I.; Blümel, J. Disentangling different modes of mobility for triphenylphosphine oxide adsorbed on alumina. *J. Chem. Phys.* **2020**, *152*, 054718.
- (8) Oprunenko, Y.; Gloriozov, I.; Lyssenko, K.; Malyugina, S.; Mityuk, D.; Mstislavsky, V.; Günther, H.; Von Firks, G.; Ebener, M. Chromium tricarbonyl complexes with biphenylene as η^6 ligand: synthesis, structure, dynamic behaviour in solid state and thermal η^6, η^6 -haptotropic rearrangements. Experimental (NMR) and theoretical (DFT) studies. *J. Organomet. Chem.* **2002**, *656*, 27–42.
- (9) Conley, M. P.; Coperet, C.; Thieuleux, C. Mesostructured Hybrid Organic-Silica Materials: Ideal Supports for Well-Defined Heterogeneous Organometallic Catalysts. *ACS Catal.* **2014**, *4*, 1458–1469.
- (10) Kharel, S.; Bhuvanesh, N.; Gladysz, J. A.; Blümel, J. New hydrogen bonding motifs of phosphine oxides with a silanediol, a phenol, and chloroform. *Inorg. Chim. Acta* **2019**, 490, 215–219.
- (11) Hilliard, C. R.; Bhuvanesh, N.; Gladysz, J. A.; Blümel, J. Synthesis, purification, and characterization of phosphine oxides and their hydrogen peroxide adducts. *Dalton Trans.* **2012**, *41*, 1742–1754. (12) Ahn, S. H.; Cluff, K. J.; Bhuvanesh, N.; Blümel, J. Hydrogen Peroxide and Di(hydroperoxy)propane Adducts of Phosphine Oxides as Stoichiometric and Soluble Oxidizing Agents. *Angew. Chem., Int. Ed.* **2015**, *54*, 13341–13345.

- (13) Arp, F. F.; Bhuvanesh, N.; Blümel, J. Hydrogen peroxide adducts of triarylphosphine oxides. *Dalton Trans.* **2019**, *48*, 14312–14325
- (14) Ahn, S. H.; Lindhardt, D.; Bhuvanesh, N.; Blümel, J. Di(hydroperoxy)cycloalkanes Stabilized via Hydrogen Bonding by Phosphine Oxides: Safe and Efficient Baeyer-Villiger Oxidants. *ACS Sustainable Chem. Eng.* **2018**, *6*, 6829–6840.
- (15) Ahn, S. H.; Bhuvanesh, N.; Blümel, J. Di(hydroperoxy)alkane Adducts of Phosphine Oxides: Safe, Solid, Stoichiometric, and Soluble Oxidizing Agents. *Chem.—Eur. J.* **2017**, 23, 16998–17009.
- (16) Arp, F. F.; Bhuvanesh, N.; Blümel, J. Di(hydroperoxy)-cycloalkane Adducts of Triarylphosphine Oxides: A Comprehensive Study Including Solid-State Structures and Association in Solution. *Inorg. Chem.* **2020**, *59*, 13719–13732.
- (17) Sommer, J.; Yang, Y.; Rambow, D.; Blümel, J. Immobilization of Phosphines on Silica: Identification of Byproducts via ³¹P CP/MAS Studies of Model Alkyl-, Aryl-, and Ethoxyphosphonium Salts. *Inorg. Chem.* **2004**, *43*, 7561–7563.
- (18) Schnellbach, M.; Blümel, J.; Köhler, F. H. The Union Carbide catalyst (Cp₂Cr + SiO₂), studied by solid-state NMR. *J. Organomet. Chem.* **1996**, 520, 227–230.
- (19) Cluff, K. J.; Schnellbach, M.; Hilliard, C. R.; Blümel, J. The adsorption of chromocene and ferrocene on silica: A solid-state NMR study. *J. Organomet. Chem.* **2013**, 744, 119–124.
- (20) Cluff, K. J.; Blümel, J. Adsorption of ferrocene on carbon nanotubes, graphene, and activated carbon. *Organometallics* **2016**, *35*, 3939–3948.
- (21) Cluff, K. J.; Blümel, J. Adsorption of Metallocenes on Silica. *Chem.—Eur. J.* **2016**, 22, 16562–16575.
- (22) Cluff, K. J.; Bhuvanesh, N.; Blümel, J. Adsorption of Ruthenium and Iron Metallocenes on Silica: A Solid-State NMR Study. *Organometallics* **2014**, *33*, 2671–2680.
- (23) Hubbard, P. J.; Benzie, J. W.; Bakhmutov, V. I.; Blümel, J. Ferrocene adsorbed on silica and activated carbon surfaces: a solid-state NMR study of molecular dynamics and surface interactions. *Organometallics* **2020**, *39*, 1080–1091.
- (24) Li, K.-T.; Yang, C.-N. Uniform rod-like self-assembly of polymer nanofibrils produced via propylene polymerization on Stober silica nuclei supported metallocene catalysts. *Mater. Today Commun.* **2019**, *19*, 80–86.
- (25) Estrada-Ramirez, A. N.; Ventura-Hunter, C.; Vitz, J.; Díaz-Barriga Castro, E.; Peralta-Rodriguez, R. D.; Schubert, U. S.; Guerrero-Sánchez, C.; Pérez-Camacho, O. Poly(n-alkyl methacrylate)s as Metallocene Catalyst Supports in Nonpolar Media. *Macromol. Chem. Phys.* **2019**, 220 (19), 1900259.
- (26) Bernardes, A. A.; Scheffler, G. L.; Radtke, C.; Pozebon, D.; dos Santos, J. H. Z.; da Rocha, Z. N. Supported metallocenes produced by a non-hydrolytic sol-gel process: Application in ethylene polymerization. *Colloids Surf. A Physicochem. Eng. Asp.* **2020**, 584, 124020.
- (27) McKenna, W. P.; Bandyopadhyay, S.; Eyring, E. M. FT-IR/PAS Investigation of Chromocene Supported on Silica. *Appl. Spectrosc.* **1984**, *38*, 834–837.
- (28) Karol, F. J.; Karapinka, G. L.; Wu, C.; Dow, A. W.; Johnson, R. N.; Carrick, W. L. *J. Polym. Sci. A1* **1972**, *10*, 2621.
- (29) Heise, H.; Köhler, F. H; Xie, X. Solid-state NMR spectroscopy of paramagnetic metallocenes. *J. Magn. Reson.* **2001**, *150*, 198–206.
- (30) Blümel, J.; Hiller, W.; Herker, M.; Köhler, F. H. Solid-State Paramagnetic NMR Spectroscopy of Chromocenes. *Organometallics* **1996**, *15*, 3474–3476.
- (31) Bakhmutov, V. I. Strategies for solid-state NMR studies of materials: from diamagnetic to paramagnetic porous solids. *Chem. Rev.* **2011**, *111*, 530–562.
- (32) Köhler, F. H.; Xie, X. Vanadocene as a temperature standard for ¹³C and ¹H MAS NMR and for solution-state NMR Spectroscopy. *Magn. Reson. Chem.* **1997**, 35, 487–492.
- (33) Pell, A. J.; Pintacuda, G.; Grey, C. P. Paramagnetic NMR in solution and the solid state. *Prog. Nucl. Magn. Reson. Spectrosc.* **2019**, 111, 1–271.

- (34) Fischer, R. A.; Nlate, S.; Hoffmann, H.; Herdtweck, E. Blümel, Two Types of Intramolecular Lewis-Base Adducts with the [2-(Dimethyl-amino)ethyl]cyclopentadienyl Ligand: Synthesis and Crystal Structures of $\{\eta^5:\eta^1\text{-}C_5H_4[(CH_2)_2NMe_2]\}\text{Ni-I}$ and $\{\eta^5:\mu\text{-}C_5H_4[(CH_2)_2NMe_2]\}\text{(Me}_3P)\text{Ni-InI}_2$. Organometallics 1996, 15, 5746–5752.
- (35) Pope, J.; Sue, H.-J.; Bremner, T.; Blümel, J. High-temperature steam-treatment of PBI, PEEK, and PEKK polymers with H_2O and D_2O : A solid-state NMR study. *Polymer* **2014**, *S5*, 4577–4585.
- (36) Pope, J. C.; Sue, H.-J.; Bremner, T.; Blümel, J. Multinuclear solid-state NMR investigation of the moisture distribution in PEEK/PBI and PEKK/PBI blends. *J. Appl. Polym. Sci.* **2015**, *1*32, 1804–1816
- (37) Ding, K.; Cullen, D. A.; Zhang, L.; Cao, Z.; Roy, A. D.; Ivanov, I. N.; Cao, D. A general synthesis approach for supported bimetallic nanoparticles via surface inorganometallic chemistry. *Science* **2018**, 362, 560–564.
- (38) Martin, B.; Autschbach, J. Temperature dependence of contact and dipolar NMR chemical shifts in paramagnetic molecules. *J. Chem. Phys.* **2015**, *142*, 054108.
- (39) Pritchard, B. P.; Simpson, S.; Zurek, E.; Autschbach, J. Computation of chemical shifts for paramagnetic molecules: a laboratory experiment for the undergraduate curriculum. *J. Chem. Educ.* **2014**, *91*, 1058–1063.
- (40) Narankiewicz, Z.; Blumenfeld, A. L.; Bondareva, V. L.; Mamedyarova, I. A.; Nefedova, M. N.; Sokolov, V. I. Molecular motions and the structure of β -cyclodextrin inclusion complexes with ferrocene, (3)-Ferrocenophane-l,3-dione and ruthenocene. *J. Inclusion Phenom. Mol. Recognit. Chem.* **1991**, *11*, 233–245.
- (41) Rouf, S. A.; Mares, J.; Vaara, J. Relativistic approximations to paramagnetic NMR chemical shift and shielding anisotropy in transition metal systems. *J. Chem. Theory Comput.* **2017**, 13 (8), 3731–3745.
- (42) Gedat, E.; Schreiber, A.; Albrecht, J.; Emmler, Th.; Shenderovich, I.; Findenegg, G. H.; Limbach, H.-H.; Buntkowsky, G. ²H-Solid-State NMR Study of Benzene-*d*₆ Confined in Mesoporous Silica SBA-15. *J. Phys. Chem. B* **2002**, *106*, 1977–1984.
- (43) Shenderovich, I. G. For Whom a Puddle Is the Sea? Adsorption of Organic Guests on Hydrated MCM-41 Silica. *Langmuir* **2020**, *36*, 11383–11392.
- (44) Stejskal, E. O.; Schaefer, J.; Sefcik, M. D.; McKay, R. A. Magic-Angle Carbon-13 Nuclear Magnetic Resonance Study of the Compatibility of Solid Polymeric Blends. *Macromolecules* **1981**, *14*, 275–279.
- (45) Meier, R.; Kahlau, R.; Kruk, D.; Rossler, E. A. Comparative studies of the dynamics in viscous liquids by means of dielectric spectroscopy and field cycling NMR. *J. Phys. Chem. A* **2010**, *114*, 7847–7855.
- (46) Kruk, D.; Mielczarek, A.; Korpala, A.; Kozlowski, A.; Earle, K. A.; Moscicki, J. Sensitivity of ²H NMR spectroscopy to motional models: proteins and highly viscous liquids as examples. *J. Chem. Phys.* **2012**, *136*, 244509.
- (47) Polimeno, A.; Freed, J. H. A many-body stochastic approach to rotational motions in liquids: complex decay times in highly viscous fluids. *Chem. Phys. Lett.* **1990**, *174*, 481–488.
- (48) Roessler, E.; Tauchert, J.; Eiermann, P. Cooperative reorientations, translation motions, and rotational jumps in viscous liquids. *J. Phys. Chem.* **1994**, *98*, 8173–8180.
- (49) Blümel, J. Reactions of Ethoxysilanes with Silica: A Solid-State NMR Study. J. Am. Chem. Soc. 1995, 117, 2112–2113.
- (50) Levenberg, K. A Method for the Solution of Certain Non-Linear Problems in Least Squares. *Quart. Appl. Math.* **1944**, *2*, 164–168.